

Biomechanical Properties of the Excised Pediatric Human Rib

K. L. Pfefferle¹, A. Litsky¹, B. Donnelly², and J. Bolte IV¹

¹The Ohio State University; ²NHTSA's Vehicle Research and Test Center

This paper has not been screened for accuracy nor refereed by any body of scientific peers and should not be referenced in the open literature.

ABSTRACT

The leading cause of death among children is traumatic injury. Injuries in which the head and abdomen are injured account for 40% of the trauma related deaths and isolated thoracic injuries account for 5% of the deaths. The initial motion of the thorax dictates the relative movement of the head and cervical vertebrae. Therefore, it is important to define the properties of the thorax to understand and predict the motion of the head and neck in traumatic injury. Further, pediatric thoracic injuries such as pulmonary contusions have been shown to occur without any rib fracture due to the increased flexibility of the developing rib cage as compared to an adult.

The material properties of the adult rib have been well documented, whereas little information is available for the mechanical properties of the pediatric rib. Currently the biomechanical values used to create the pediatric anthropomorphic testing device (ATD) are obtained from scaling the adult properties purely based on size. Accurate data defining the material properties of the pediatric rib will improve analytical modeling results and provide valuable information for child dummy design.

To date, The Ohio State University Injury Biomechanics Research Laboratory has tested 48 rib specimens from 13 pediatric human subjects with ages ranging from 1 day to 6 years of age. Each rib specimen was tested in three-point bending and analyzed for stiffness, Young's modulus, peak force and yield stress. These material properties were analyzed both at biological age and at a corrected "age" based on the National Growth Charts. The findings have been compared to published adult rib properties.

INTRODUCTION

The leading cause of death among children is traumatic injury. Injuries in which the head and abdomen are injured account for 40% of trauma related deaths and isolated thoracic injuries account for 5% of these deaths (Bliss and Silen, 2002). As the ribs become loaded, the displacement is transferred to the spine. As a result, the initial motion of the thorax dictates the relative movement of the neck and cervical vertebrae. Therefore, it is important to define the properties of the thorax to understand and predict the motion of the head and neck in traumatic injury. Pediatric thoracic injuries such as pulmonary contusions have been shown to occur without any rib fracture. This is thought to occur because of the increased flexibility of the developing rib cage as compared to an adult (Bliss and Silen, 2002).

The material properties of the adult rib have been well documented (Kemper et al., 2007; Yoganandan and Pintar, 1998; Cormier et al., 2005), whereas little information is available for the mechanical properties of the pediatric rib. Yoganandan and Pintar tested adult ribs quasi-statically in three point bending. Yoganandan et al. reported an average yield force of 145N and an average modulus of elasticity of 2102 N/mm² for adult rib levels 7 and 8. Cormier et al. tested adult ribs dynamically at a rate of 500-1000 mm/s in three point bending. Cormier et al. reported an average peak force of 164N and an average modulus of elasticity 24,000 N/mm². Kemper et al. tested adults ribs dynamically at a rate of 172 mm/s. Kemper et al. reported modulus of 21,000 N/mm² in ribs from the lateral region of the rib cage and 18,900 N/mm² in ribs taken from the anterior location of the rib cage.

Currently, the biomechanical values used to create the pediatric anthropomorphic testing device (ATD) are obtained from scaling adult and animal surrogate properties purely based on mass and length. This method of scaling is not desired for optimal design of the pediatric ATD, because the pediatric rib cage differs from the adult rib cage in material composition (Takahashi and Frost, 1966). The heart takes up more area in the pediatric thorax and the overall shape of the pediatric thorax differs from the adult thorax. Accurate data defining the material properties of the pediatric rib will improve analytical modeling results and provide valuable information for child dummy design. The testing protocol and apparatus developed by Xavier (2006) was used in this study in an effort to determine the material properties of pediatric human ribs.

METHODS

Objective

The objectives of this study are to:

- Develop an experimental technique to accurately measure the mechanical properties of the pediatric human rib,
- Examine the pediatric rib material properties as a function of age.

Subject Collection and Preparation

The collection of pediatric rib specimens for this study was approved by the Institutional Review Board at Nationwide Children's Hospital in Columbus, Ohio (IRB submission # IRB05-00035; Columbus Children's Hospital Federalwide Assurance # FWA00002860). The patient population inclusion age was specified to be full-term infants through subjects of 21 years of age. The exclusion criteria included:

- Patients who experienced significant chest trauma (except CPR) prior to death,
- Conditions such as rickets, osteogenesis imperfecta, osteoporosis, and any other genetic, metabolic, or acquired disease affecting bone structure or mineral content,
- Patients receiving medication or treatment affecting bone density (ex: chronic steroid use),
- HIV/AIDS, Hepatitis B patients (infectious risk).

The samples were collected between rib levels 5 through 8 with 1-2 ribs per each hemi-thorax for a total of 2-4 ribs per subject. The locations of the rib specimens are shown in Figure 1a. Each specimen was removed from the sternum to the mid-clavicular line, then wrapped in saline soaked gauze and frozen at -17° C. A total of 48 ribs from 13 subjects were collected with ages ranging from 1 day to 72 months old. The age of the subjects is shown in Figure 1b. The age of subjects 3 and 8 were both 1 day old.

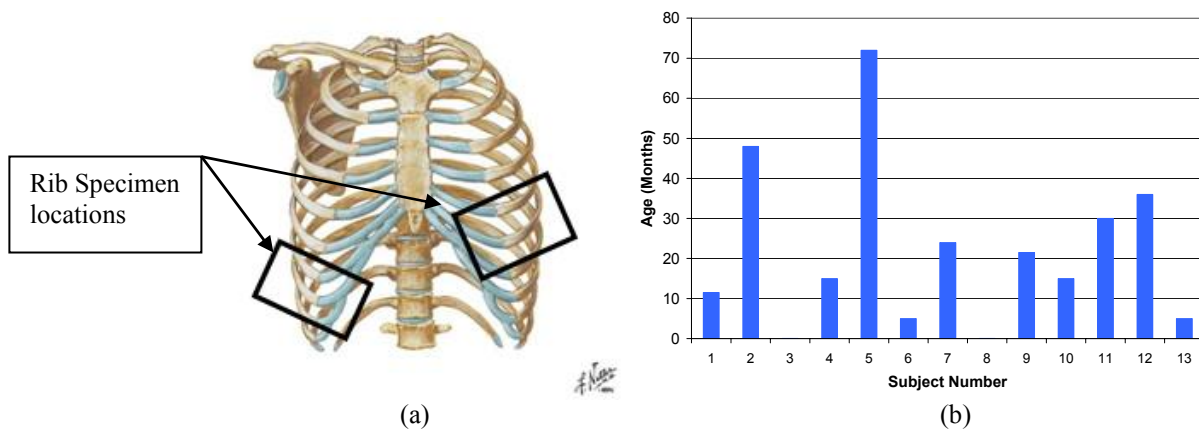


Figure 1: (a) Rib specimen locations, (b) Subject Age (months).

On the day of testing, specimens were allowed to thaw and all soft tissue was removed. Two ink markers were placed approximately 180° apart at the mid-span length as shown in Figures 2a and 2b.

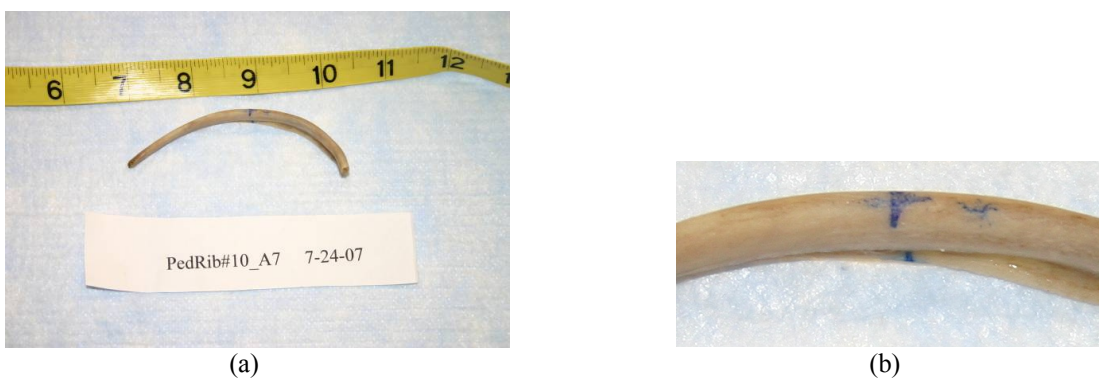


Figure 2: (a) Ribs specimen with soft tissue removed, (b) Ink maker on pediatric rib.

Specimens were then placed in a foam holder containing a radio-opaque marker as shown in Figure 3. The ribs were oriented as to ensure the ink markers on the ribs and the radio-opaque marker in the foam block were in the same vertical plane. The foam holders were then secured to a board to ensure a fixed orientation of the ribs during CT imaging.

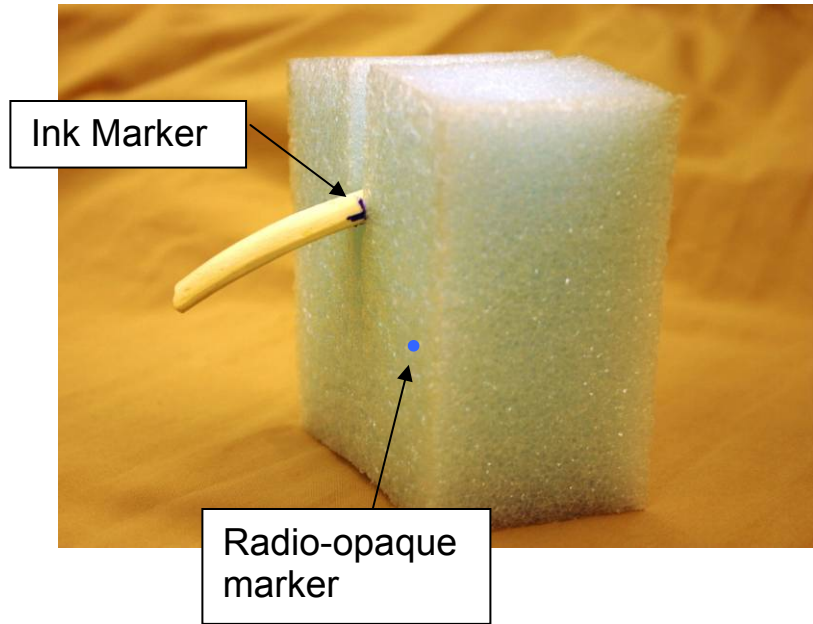


Figure 3: Pediatric rib in foam holder.

The vertical height of each ink marker was then recorded with:

- D_1 = the vertical height of marker one
- D_2 = the vertical height of marker two
- h = the distance between the two ink markers
- θ_1 = the angle the markers make from the horizontal plane

From these measurements, the angle the rib markers make from the horizontal plane could be determined as shown in Figure 4.

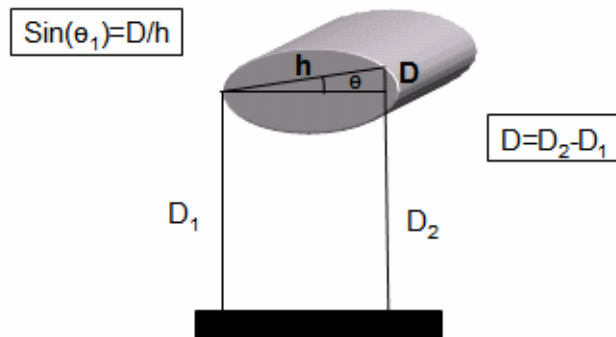


Figure 4: Pre-CT measurements.

Cross section CT images were then collected at 0.6 mm intervals. The images were examined to find the image containing the radio-opaque marker, which corresponds to the cross section containing the ink rib markers. From the pre-CT measurement it is known that the ink markers make an angle θ_1 from the horizontal plane as shown in Figure 5(a). The CT cross section image can now be rotated θ_1 degrees as seen in Figure 5(b). The ink makers are now parallel with the horizontal plane in Figure 5(b) and the exact orientation of the rib cross section is now known. The yellow line in Figures 5(a) and 5(b) indicate the angle at which the ink markers are aligned.

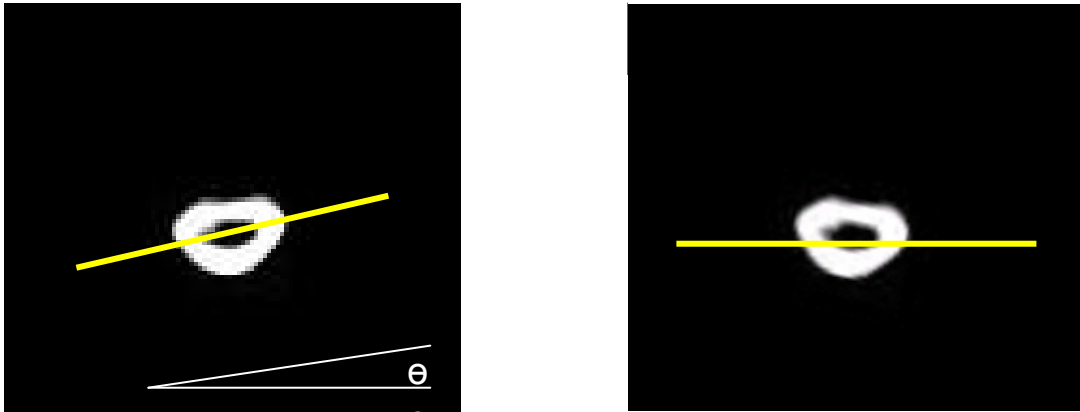


Figure 5: (a) CT cross section containing radio-opaque marker, (b) CT cross section rotated θ_1 degrees.

Test Setup

An adjustable span three-point bending apparatus was developed to accommodate variable length specimens as shown in Figure 6. The testing was completed in The Ohio State University Orthopaedics Biomaterials Laboratory. The top portion of the three-point bend fixture was screwed into the cross-head of an MTS Material Testing System[®] (MTS Systems Corporation; Eden Prairie, MN). Each rib specimen was loaded at the location of the ink markers at a rate of 2.5 mm/min. The displacement rate for this study of 2.5 mm/min was the same as that used by Yoganangan and Pintar. It was observed that rotation of the rib occurred during load. Therefore the vertical height of each marker was recoded after a 5 N preload and a second time after 0.75 mm of displacement. Loading of the ribs then continued until failure.

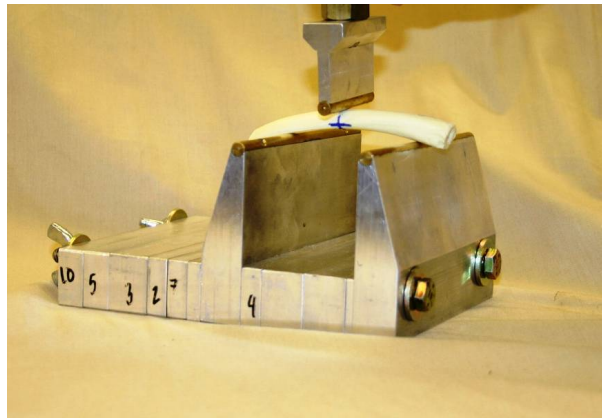
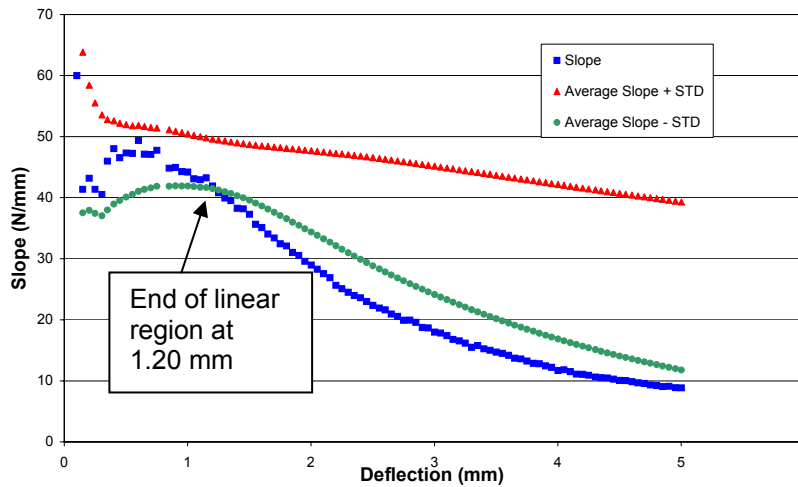


Figure 6: Three-point test setup.

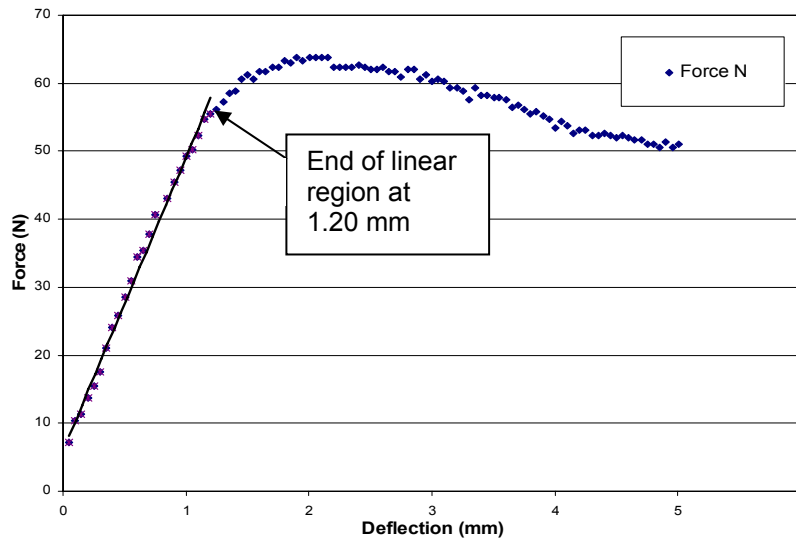
Using the measurements taken at 0.75 mm of displacement, the angle θ_2 could be calculated. The orientation of the rib cross section CT was determined as previously described. The CT image was then rotate θ_2 degrees. From the angle θ_2 , the orientation of the rib during loading could be determined. With the CT image in the exact orientation of the rib during testing, the software program ImageJ version 1.36b with the macro MomentMacroJ v1.2 (developed by Dr. Chris Ruff of Johns Hopkins University) was used to calculate the bending moment of inertia.

Data Analysis

The force of the center loading head was recorded using a load cell. The force of the load cell was then plotted against the displacement measured by the MTS machine. The end of the linear portion of the force deflection curve was defined as the point at which the average slope, calculated to that data point, deviated above or below the mean of all preceding calculated average slopes by more than one standard deviation. As seen in Figure 7a, the average slope exceeds the mean of all preceding average slopes by more than \pm one standard deviation at 1.2 mm of displacement, defining the linear portion of the force-deflection curve for this specimen to be from 0 mm to 1.2 mm of displacement. The newly defined linear portion of the force deflection curve is shown in Figure 7b.



(a)



(b)

Figure 7: (a) Average slope exceeds the slopes \pm one STD, (b) Linear portion of force deflection curve.

The stiffness was defined as the slope of the linear region of the force-deflection curve. After determining the linear region of the force deflection curve, the data was fit with a linear regression. Next, a power curve was fit from the maximum force to 90% of the maximum force. The force corresponding to the displacement point at which the linear fit and power fit intersect was defined as the yield force. The method to determine the yield force was adapted from that developed by Datsko (as cited in Margulies and Thibault, 2000).

The modulus of elasticity (Young's modulus) is given by

$$E = \left(\frac{F}{\omega} \right) \frac{L^3}{48I} \quad (\text{eq 1})$$

where E is the modulus of elasticity, L is the span length of the test fixture, $\left(\frac{F}{\omega} \right)$ is the stiffness, and I is the moment of inertia. This equation is derived from beam theory for a simply supported beam with a load at mid-span (Stevens, 1987). In order for the analysis to be valid several assumptions were made:

- General equations for analysis of three-point bending behavior are valid only before yielding occurs, and the material remains linearly elastic up until the point of failure (Currey, 2002; Turner and Burr, 1993).
- The beam is a straight beam; ie, the ratio of the radius of curvature to the depth of the beam is greater than five ($R/d > 5$) (Boresi et al., 1993).
- Error from the flexure formula is negligible if the test specimen is sufficiently long and slender; i.e., the ratio of the span of the beam length to the maximum cross-sectional dimension of the beam must be larger than five ($L/d > 5$) (Boresi et al., 1993). This minimizes the effects of the induced transverse shear stresses from three-point bending, as there are no shear stresses in pure bending (Carter, 1985; Stevens, 1987).
- Moduli remain constant throughout the test specimen (Cowin, 2001).
- The neutral and centroidal axes coincide (Biewener, 1992; Cowin, 2001). The first moment of area about the neutral axis is equal to zero.
- Material is homogeneous and isotropic (Stevens, 1987).

The pediatric ribs tested did meet the criteria of $R/d > 5$ as well as $L/d > 5$ but it should be noted that the moduli is not constant throughout the specimen nor is the material homogeneous or isotropic.

During the collection of the specimens it was noticed that several of the subjects were well below the 5th percentile for their height and weight according to CDC growth charts. It was reported by Cardoso (2006) that bone developmental age is sensitive to environmental influences, specifically socioeconomic influences such as the effects of nutrition, disease and social status. Since the subjects for this study were exposed to the environmental influence of disease, it is thought that their bone development may be delayed. Scheuer and Black (2000) reported that long bone growth is not a good predictor of actual (biological) age but a better measure of bone development and maturity. Therefore, it is thought that height, representing long bone growth, may be a better predictor of bone development than the subject's biological age. Thus, all subjects were analyzed for both biological as well as a "developmental age". The "developmental age" was determined by assigning the age at which the height corresponds to the 50th percentile on the CDC growth chart. The newly assigned "developmental ages" for each subject are shown in Figure 8. It should be noted that the height for subject 12 was unavailable therefore no "developmental age" was assigned. The data for subjects 3 and 8 is shown in all plots but was not included in any of the data analysis.

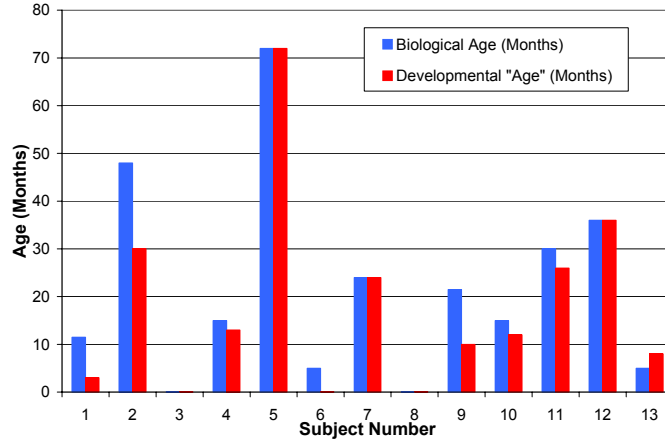


Figure 8: "Developmental Age".

RESULTS

Test Results

The bending moment of inertia was plotted against the "developmental age" in Figure 9. It can be seen that there is considerable scatter throughout the data. The scatter is thought to be attributed to geometric variation between rib levels as well as variation along the rib itself. This geometric variation was also reported by Kemper et al. (2007).

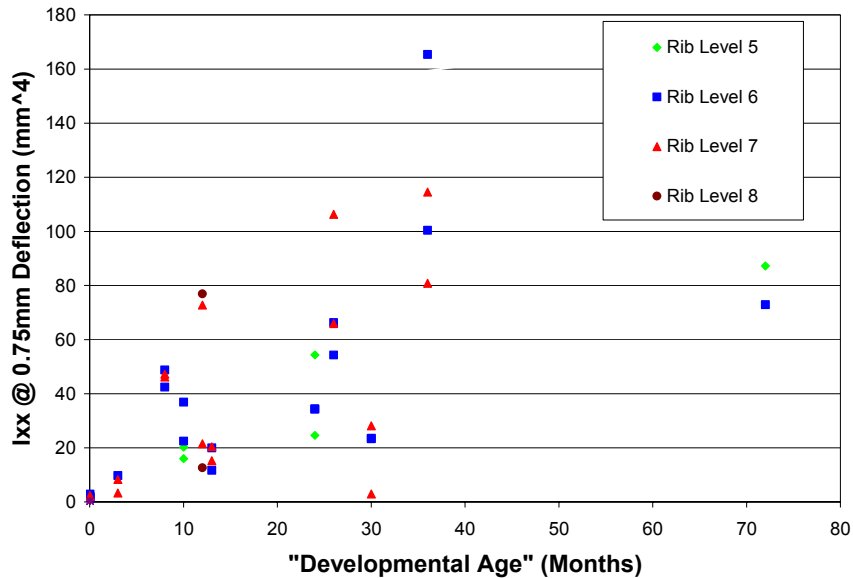


Figure 9: Bending moment of inertia calculated from rib orientation at 0.75mm of Displacement versus "Developmental Age".

The rib stiffness, defined as the slope of the linear portion of the force-deflection curve, was plotted against both the biological age and “developmental age” as seen in Figures 10 and 11, respectively. The data in Figures 10 and 11 have been fitted with a power curve. Notice that the R^2 value of 0.7857 in Figure 11 is considerably greater than the value of 0.2892 as seen in Figure 10.

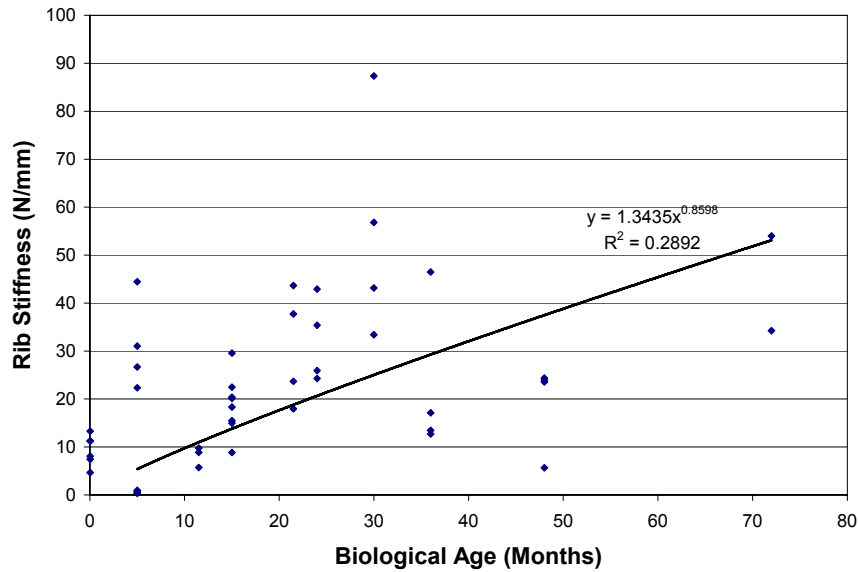


Figure 10: Rib stiffness (N/mm) versus Biological Age (months).

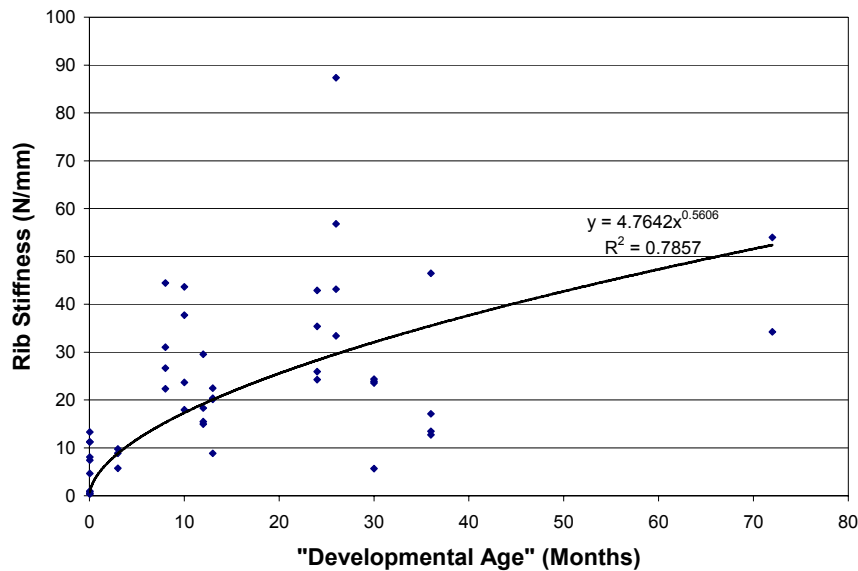


Figure 11: Rib stiffness (N/mm) versus “Developmental Age” (months).

The yield force (N), calculated using the method previously described, has been plotted against the biological age and the “developmental age” in Figures 12 and 13, respectively. The data in Figures 12 and 13 have been fitted with a power curve. Notice that the R^2 value of 0.8518 in Figure 13 is considerably greater than the value of 0.4217 as seen in Figure 12. The adult yield force data obtained by Yoganandan and Pintar as well as the adult peak force data obtained by Cormier et al. has been plotted in Figure 13. It can be seen in Figure 13 that the pediatric data is below but approaching the adult data, as would be expected.

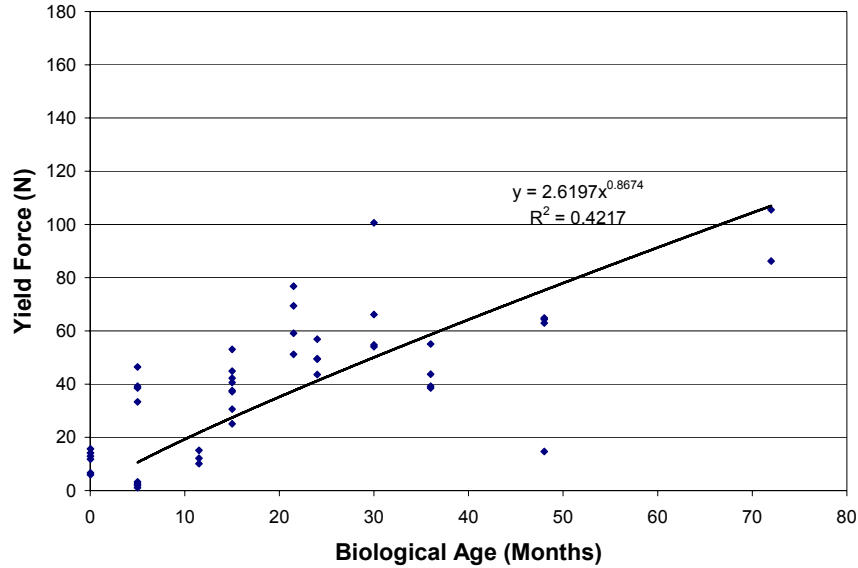


Figure 12: Yield force (N) versus Biological Age (months).

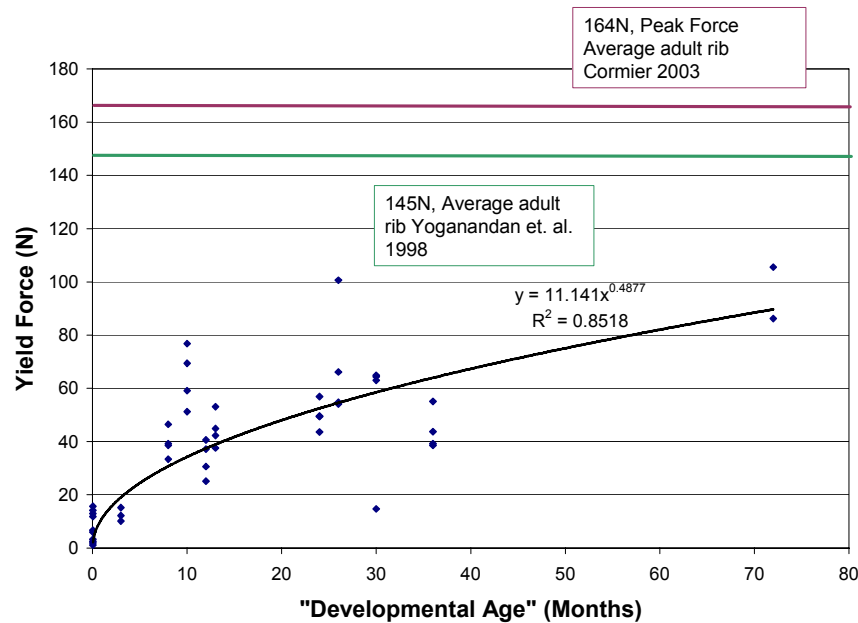


Figure 13: Yield force (N) versus "Developmental Age" (months) with adult data.

The elastic modulus (N/mm^2) was plotted against both the biological age and "developmental age" as seen in Figures 14 and 15, respectively. The data in Figures 14 and 15 have been fitted with a power curve. Notice that the R^2 value of 0.494 in Figure 14 is greater than the value of 0.4106 as seen in Figure 15. The adult elastic modulus data obtained by Yoganandan and Pintar (1998) as well as the data obtained by Cormier et al. (2005) has been plotted in Figure 15. It can be seen in Figure 15 that the pediatric data is well below that obtained by Cormier et al. but is equal to or greater than that obtained by Yoganandan and Pintar.

Cormier attributed this large difference in adult rib elastic modulus to the visco-elastic effects in the dynamic versus static testing.

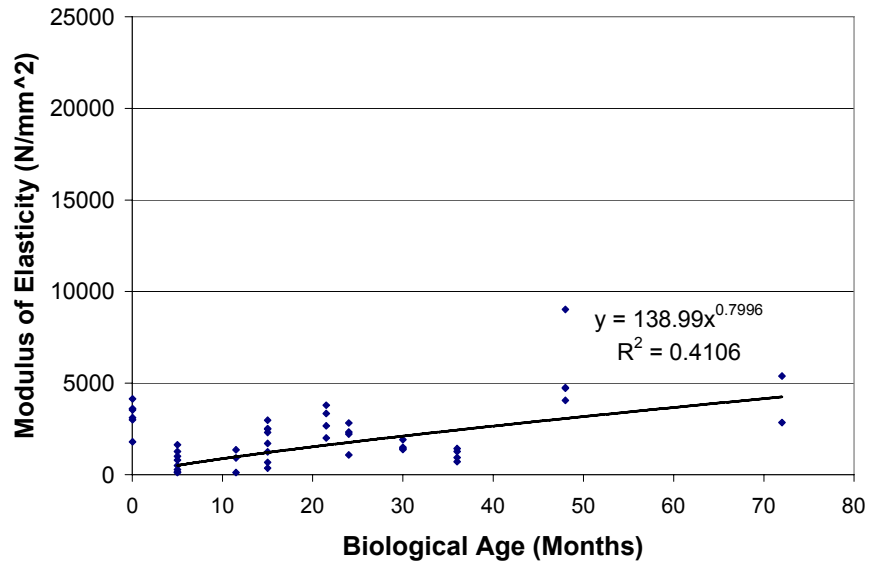


Figure 14: Modulus of elasticity (N/mm²) versus Biological Age (months).

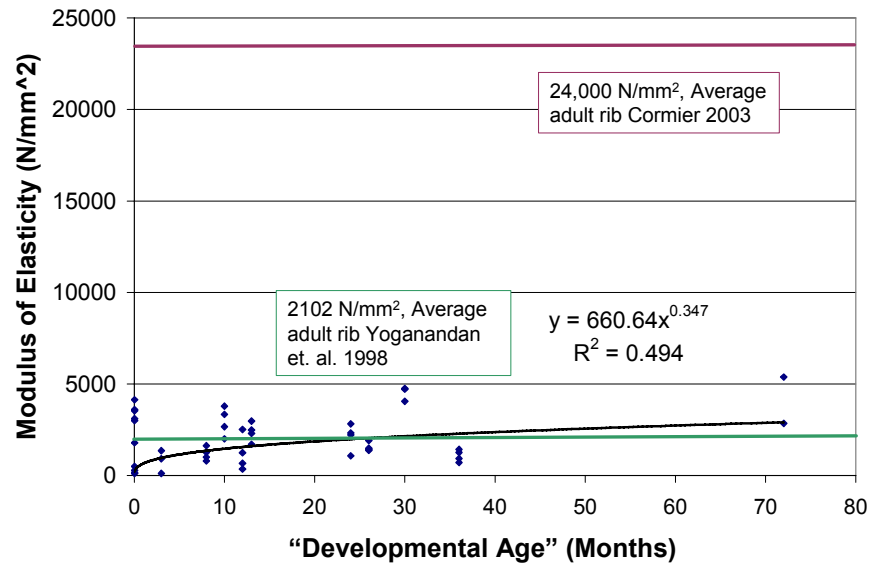


Figure 15: Modulus of Elascity (N/mm²) versus "Developmental Age" (months) with adult data.

CONCLUSIONS

The use of CT cross section images and ImageJ software provides an accurate and non-destructive method to determine the bending moment of inertia in the exact orientation the rib was in during bending. The accurate calculation of the bending moment of inertia allows the material properties of the pediatric rib to be determined.

As shown in the results section, the “developmental age” appears to be a better predictor of rib material properties than the actual biological age. In an effort to better define the material properties of the pediatric rib, more testing is necessary. The results of this study have been compared to the adult rib data and are shown in Table 1.

Table 1. Summary of Results.

Age (Years)	Modulus of elasticity (N/mm ²)	Yield Force (N)
1 ("Developmental age")	1,565	37
3 ("Developmental age")	2,290	64
Adult (Kemper 2007)	21,100	N/R
Adult (Yoganandan 1998)	2,102	145
Adult (Cormier 2005)	24,000	164

The limitations of this study should be noted. It is unfortunate that the medical history of the subjects is unknown. Therefore, it is unknown whether the subjects suffered from a chronic illness that may have delayed their rib development or if they died from an acute illness. There remains a degree of subjectivity in the threshold selection in the imageJ software. The inconsistency in the anterior/posterior location of the rib specimen collection between subjects may have led to further variation.

Alternative methods to determine the subject bone development will be explored in the future. An in-situ rib testing device will be manufactured to allow for rapid material testing. Finally, it is desired to conduct non-destructive intact pediatric thorax stiffness measurements.

ACKNOWLEDGEMENTS

This work was completed under NHTSA contract DTNH22-03-D-08000. The authors would like to thank Angela Xavier from The Ohio State University, Rod Herriott from TRC and Gary Smith MD, Peter Baker MD and Emily Chenever from Nationwide Children’s Hospital for their expertise and assistance in this project.

REFERENCES

- BIEWENER, A. A., ed. (1992). *Biomechanics: Structures and Systems. A Practical Approach*. Oxford University Press, Oxford.
- BLISS, D. and SILEN, M. (2002). Pediatric thoracic trauma. *Critical Care Medicine*, 30(11 Suppl.): S409-15, November.
- BORESI, A. P., SCHMIDT, R. J., and SIDEBOTTOM, O. M. (1993). *Advanced Mechanics of Materials*, 5th ed. John Wiley & Sons, Somerset, NJ.
- CARDOSO, H. (2006). Environmental Effects on Skeletal Versus Dental Development: Using a Documented Subadult Skeletal Sample to Test a Basic Assumption in Human Osteological Research, *American Journal of Physical Anthropology*, DOI 10.1002/ajpa.20482, October.
- CORMIER, J. M., STITZEL, J. D., DUMA, S. M., and MATSUOKA, F. (2005). Regional variation in the structural response and geometrical properties of human ribs, *AAAM*, 49:153-70.
- COWIN, S. C. (2001). *Bone Mechanics Handbook*, 2nd ed. CRC Press, New York, NY.
- CURREY, J. D. (2002). *Bones: Structure and Mechanics*. Princeton University Press, Princeton, NJ.
- KEMPER, A., MCNALLY, C., PULLINS, C., FREEMAN, L., and DUMA, S. (2007). The Biomechanics of Human ribs: Material and Structural Properties from Dynamic Tension and Bending Tests; Stapp Car Crash Journal, Vol 51, October.
- MARGULIES, S. S. and THIBAUT, K. L. (2000). Infant skull and suture properties: Measurements and implications for mechanisms of pediatric brain injury. *Transactions of the ASME: Journal of Biomechanical Engineering*, 122: 364-71, August.
- SCHEUER, L. and BLACK, S. (2000). *Development Juvenile Osteology*, Academic Press.
- STEVENS, K. K. (1987). *Statics and Strength of Materials*, 2nd edition. Prentice-Hall, Inc., Englewood Cliffs, NJ.
- TAKAHASHI H. and FROST H. M. (1966). Age and sex related changes in the amount of cortex of normal human ribs. *Acta orthopædica Scandinavia*, 37: 122-30.
- TURNER, C. H. and BURR, D. B. (1993). Basic biomechanical measurements of bone: A tutorial. *Bone*, 14: 595-608.
- XAVIER, A. (2006). Determination of the Material Properties of the Pediatric Rib, Masters Thesis, The Ohio State University.
- YOGANANDAN, N. and PINTAR, F. A. (1998). Biomechanics of human thoracic ribs. *Transactions of the ASME: Journal of Biomechanical Engineering*, 120: 100-4, February.

DISCUSSION

PAPER: **Biomechanical Properties of the Excised Pediatric Human Rib**

PRESENTER: ***Kiel Pfefferle, The Ohio State University***

QUESTION: *Richard Kent, UVA*

Good work. This is very much needed. I have one question: How did you get the modulus of elasticity from your tests?

ANSWER: You mean the equation?

Q: Yes, just how did you determine modulus of elasticity from the 3-point bending tests?

A: The slope—It was the slope of our linear portion times L^2 divided by $48I$.

Q: Okay. So it's a Linear Beam Theory sort of thing.

A: Oh, correct. Yes.

Q: Okay. So, one thing you—and I think—It looked like you were taking the neutral axis as being orthogonal to the loading vector. Is that right? As you were rotating that CT image around, how were you defining the neutral axis in order to get that value of moment of inertia?

A: That was actually computed in the software program.

Q: Right, and it's defined as being orthogonal to the loading vector. The force vector's coming straight.

A: Correct. Correct.

Q: Okay. So you might want to double-check that because if you have an asymmetric cross-section like that, the neutral axis may not necessarily be orthogonal to the loading vector even though you're pushing straight down.

A: Okay.

Q: If you don't have a perfectly symmetric cross-section, that thing can rotate and so that might change your values. So it's something to look at.

A: Okay. Thank you.

Q: *Andrew Kemper, Virginia Tech*

I have a couple questions. One: You didn't mention anything about maintaining specimen hydration, which has been shown to have a large influence on the material response of bone. Did you maintain—Spray—Soak it in saline, spray it during testing or anything like that?

A: We tried to keep the rib soaked in, wrapped in saline as long as possible, and then we took them out of saline and placed them on bending and then tested them.

Q: Okay.

A: Does that answer your question?

Q: Yes. And then, you have all the CT images. Did you obtain any bone mineral densities from those? Because I would assume that, you know, as the bone starts to calcify more, that would have a stronger indication of bone strength than, say, developmental age?

A: Correct. No, we did not. Unfortunately, we do not have any bone mineral densities and that's something we want to look into to better quantify the development.

Q: Thank you.

Q: *Guy Nusholtz, DaimlerChrysler*

Can you go back to the curve that you generate your modulus and your yield?

A: This one?

Q: No, no. Keep going. Keep going. Your defining curve. There you go! Got it. That curve sort of gives an indication of something other than elastic plastic, which is the model that you're using. Have you considered another type of idealization of paradigm? It looks more like a material that's slowly breaking up and fracturing, sort of like a composite or something else. So you may find that there might be a better idealization for that type of curve than trying to do it with elastic plastic. Have you thought about doing that or are you just sort of stuck with the standard steel-type stuff?

A: We haven't—I guess we haven't thought about doing that. That's something we could look into.

Q: Yes. Because typically if you're going to bend bone—It could be, in fact, just a local effect from your indenter going into the bone or it could be actually something which is a characteristic of the rib: that you're slowly breaking fibers or breaking parts of it and you're just making the strength eventually until it eventually falls. And then when you go all the way through, it breaks off. So you might want to look at considering a different model than what you've got there.

A: Okay.

Q: And one other quick question: What's the cause of that rise in the beginning between zero and the first maybe 100th of a millimeter? So if I draw that line, it doesn't go through zero, but I assume something must be happening in the very beginning.

A: There's a 5 Newton preload.

Q: Okay. Thank you.

Q: *Gunter Siegmund, MEA Forensic*

I'm going to ask you the exact same question except for the other graphs. It looked to me that all the graphs were forced through zero and I'm just wondering why you did that on your stiffness versus developmental age.

A: We have, I guess, played around with a couple different fitting techniques and this seems to be the largest R^2 value and are aware that it is forcing zero, and we're open to suggestions on anything else that might possibly be a better fit.

Q: It's just you might be dropping some of your R^2 values by forcing it through zero. So unless you've got a physical reason to do that, you might want to watch that constraint.

A: Okay.

Q: *Jeff Crandall, UVA*

Just a comment: You mentioned you couldn't find any pediatric studies that had been done on ribs. And in 1980, Stuarts published something at STAPP, which had pediatric data, both static and dynamic. So you might want to compare to those.

A: Okay.

Q: *Kristy Arbogast, Children's Hospital of Philadelphia*

One of the things that changes in pediatric development is the angle the rib makes with the sternum because of the sternal development. And so, I wonder, within the age range that you've examined, whether differences are not only mechanical properties differences, but they're also structural difference of how the rib is loading. It might be useful to look at some whole-body CTs through your age range and just examine the geometry that the ribs make with the sternum through that age range.

A: Sure. Thank you.